Efficiency Enhancement of Organic Photovoltaics Enabled by Introducing Simple-structured Benzo[1,2-b:4,5-b']dithiophene Based Large-bandgap Small Molecules as Third Components

Huanran Feng[a,*], Zhihui Liu[a], Yinhui Bao[a], Baofeng Zhao[b], Baohua Wu[c], ZhaoZhao Bi[c], Weiwei Wu[a], Wei Ma[c,*], Chao Gao[b,*]

[a]School of Advanced Materials and Nanotechnology, Interdisciplinary Research Center of Smart Sensors, Xidian University, Shaanxi, 710126, People's Republic of China

[b]Xi'an Key Laboratory of Liquid Crystal and Organic Photovoltaic Materials, State Key Laboratory of Fluorine & Nitrogen Chemicals, Xi'an Modern Chemistry Research Institute, Xi'an, People's Republic of China

[c]State Key Laboratory for Mechanical Behavior of Materials & Frontier Institute of Science and Technology, Xi'An Jiaotong University, Xi'an 710049, People's Republic of China

Email addresses: hrfeng@xidian.edu.cn (H. F.); msewma@xjtu.edu.cn (W. M.); chaogao1974@hotmail.com (C. G.)

Experiment Details:

Materials and synthesis. Donor polymer PM6 and Y6 was purchased from Solarmer Materials, Inc. 4,8-bis(5-(2-ethylhexyl)thiophen-2-yl)benzo[1,2-b:4,5-b']dithiophene-2,6-dicarbaldehyde was prepared according to the literature.[1] The solvents were purified and dried according to standard procedures. The other materials were common commercial level and used as received.

Synthesis of BR-RD

BT-2CHO (200.0 mg),3-Butylrhodanine and piperidine (0.3 mL) were dissolved in chloroform (45 mL). The reaction was stirred at 65 °C for several hours with process was monitored by TLC. After reaction, the mixture was concentrated. The residue was purified by silica gel column chromatography (petroleum ether/dichloromethane=1:1 v/v) to obtain a dark red solid (52%). ^{1}H NMR (400 MHz, CDCl3): δ=7.95 (s, 2H), 7.9 (s, 2H), 7.33 (d, 2H), 6.97 (d, 2H), 4.12-4.1 (m, 4H), 2.94-2.92 (d, 4H), 1.7 (m, 2H), 1.56-1.37 (m, 26H), 1.00-0.93 (m, 16H). ^{13}C NMR (151 MHz, CDCl3) δ 192.33, 167.34, 147.29, 141.80, 139.65, 137.38, 135.40, 131.25, 128.47, 125.97, 125.62, 125.39, 124.71, 44.72, 41.49, 34.32, 32.53, 29.06, 28.93, 25.76, 23.06, 20.07, 14.22, 13.68, 10.97.MS (MALDI-TOF): calcd. for $C_{50}H_{60}N_2O_2S_8$ $[M]^+$, 976.2420; found, 976.2842.

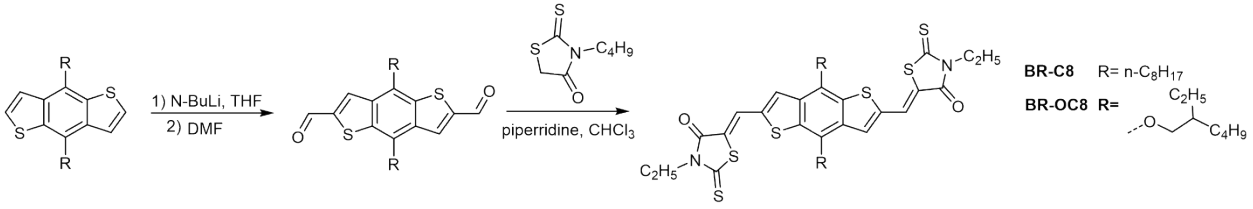

Figure S1. Synthesis route of BR-C8 and BR-OC8.

Synthesis of OC8-CHO

BDT-OC8 (200 mg) and 40 mL anhydrous THF were added to a 100 mL double-mouth flask, cooled to -78 ℃, and n-butyllithium (2.4 M) was slowly added in drops and stirred for 2 hours. Then heat to -30 ℃ and stir for 0.5 hours. After adding DMF, the solution was stirred for another 2 hours. Then slowly bring the solution to room temperature and stir overnight. The mixture was extracted with dichloromethane and water, and the organic layer was dried with anhydrous sodium sulfate and filtered. After solvent removal, the residue was purified by column chromatography. Orange solid OC8-CHO (100 mg, 45%) was obtained. ^{1}H NMR (400 MHz, $CDCl_3$): δ= 10.14 (s, 2H), 8.18 (s, 2H), 4.28-4.27 (m, 4H), 1.87-1.83 (m, 2H), 1.70-1.54 (m, 16H), 1.03-0.88 (m, 12H). ^{13}C NMR (151 MHz, $CDCl_3$) δ 184.56, 147.19, 144.32, 133.51, 131.08, 130.94, 40.76, 30.44, 29.79, 29.24, 23.89, 23.15, 14.20, 11.36. MS (MALDI-TOF): calcd. for $C_{28}H_{38}O_4S_2$ $[M]^+$, 502.2212; found, 503.2300.

Synthesis of BR-OC8

OC8-CHO (200 mg), 3-ethyl rhodanine and piperidine (0.3 mL) were dissolved in chloroform (45 mL). The reaction was stirred at 65°C for several hours with process was monitored by TLC. After reaction, the mixture was concentrated. The residue was purified by silica gel column chromatography (petroleum ether/dichloromethane=3:1 v/v) to obtain a dark red solid (125mg, 40%). 1H NMR (400 MHz, CDCl3): δ= 7.94 (s, 2H), 7.74 (s, 2H), 4.22 (d, 8H), 1.86-1.57 (m, 10H), 1.57-1.43 (m, 8H), 1.33-1.25 (m, 6H), 1.07-1.06 (m, 6H), 1.04-0.98 (m, 6H). 13C NMR (101 MHz, CDCl3) δ 192.01, 167.23, 145.67, 138.53, 132.87, 131.74, 127.84, 125.31, 124.89, 40.76, 40.16, 30.54, 29.79, 29.34, 23.93, 23.27, 14.35, 12.39, 11.46. MS (MALDI-TOF): calcd. for C38H48N2O4S6[M]+, 788.1938; found, 789.2822.

Synthesis of C8-CHO

BDT-C8 (200 mg) and 40 mL anhydrous THF were added to a 100 mL double-mouth flask, cooled to -78℃, and n-butyllithium (2.4 M) was slowly added in drops and stirred for 2 hours. Then heat to -30 ℃ and stir for 0.5 hours. After adding DMF, the solution was stirred for another 2 hours. Then slowly bring the solution to room temperature and stir overnight. The mixture was extracted with dichloromethane and water, and the organic layer was dried with anhydrous sodium sulfate and filtered. After solvent removal, the residue was purified by column chromatography. Golgen solid C8-CHO (89 mg, 40%) was obtained. ^{1}H NMR (400 MHz, $CDCl_3$): δ= 10.17 (s, 2H), 8.20 (s, 2H), 3.24-3.22 (m, 4H), 1.82-1.25 (m, 24H), 0.89-0.86 (m, 6H). ^{13}C NMR (151 MHz, $CDCl_3$) δ 184.74, 144.47, 139.95, 137.78, 133.34, 132.51, 33.37, 31.93, 30.06, 30.02, 29.51, 29.29, 22.72, 14.17. MS (MALDI-TOF) :calcd. for $C_{28}H_{38}O_2S_2[M]^+$, 470.2313; found, 470.1121.

Synthesis of BR-C8

C8-CHO (200 mg), 3-ethyl rhodanine and piperidine (0.3 mL) were dissolved in chloroform (45 mL).The reaction was stirred at 65°C for several hours with process was monitored by TLC. After reaction, the mixture was concentrated. The residue was purified by silica gel column chromatography (petroleum ether/dichloromethane=3:1 v/v) to obtain a dark red solid (122mg, 38%).^{1}H NMR (400 MHz, $CDCl_3$): δ= 8.0 (s, 2H), 7.75 (s, 2H), 4.23-4.20 (m, 4H), 3.18-3.16 (m, 4H), 1.82-1.78 (m, 4H), 1.56 (s, 6H), 1.33-1.28 (m, 20H), 0.98-0.87 (m, 6H). ^{13}C NMR (151 MHz, $CDCl_3$) δ 192.27, 167.27, 140.62, 138.74, 137.21, 131.36, 129.72, 125.73, 124.58, 40.12, 33.62, 31.99, 30.03, 29.86, 29.56, 29.32, 22.77, 14.22, 12.39. MS (MALDI-TOF):calcd. for $C_{38}H_{48}N_2O_2S_6[M]^+$, 756.2040; found, 755.1719.

Measurements and Instruments.

The ^{1}H and ^{13}C NMR spectra were taken on a Bruker AV400 spectrometer. Matrix assisted laser desorption/ionization time-of-flight (MALDI-TOF) mass spectrometry was performed on a Bruker Autoflex III instrument. Electrospray ionization mass spectrometry (ESI-MS) were performed on a Thermo-Finnigan LCQ-advantage instrument. The thermogravimetric analysis (TGA) was carried out on a NETZSCH STA 409PC instrument under purified nitrogen gas flow. The heating rate for TGA testing is 10 °C·min^{-1}. Ultraviolet-visible (UV−vis) spectra was obtained with a JASCO V-570 spectrophotometer. Cyclic voltammetry (CV) experiments were performed with a CHI660E microcomputer-based electrochemical analyzer in dichloromethane solutions. All measurements were carried out at room temperature with a conventional three-electrode configuration employing a glassy carbon electrode as the working electrode, a saturated calomel electrode (SCE) as the reference electrode, and a Pt wire as the counter electrode. Tetrabutylammonium phosphorus hexafluoride (n-Bu_4NPF_6, 0.1 M) in dichloromethane was used as the supporting electrolyte, and the scan rate was 100 mV·s^{-1}. The HOMO and LUMO energy levels were calculated from the onset oxidation potential and the onset reduction potential, using the equation $E_{HOMO} = -(4.80 + E_{ox}^{onset})$, $E_{LUMO} = -(4.80 + E_{re}^{onset})$.

Atomic force microscope (AFM) investigation was performed using Bruker MultiMode 8 in tapping mode. The transmission electron microscopy (TEM) investigation was performed on Philips Technical G2 F20 at 200 kV. The specimen for TEM measurement was prepared by spin casting the blend solution on ITO/PEDOT:PSS substrate, then floating the film on a water surface, and transferring to TEM grids. Grazing Incidence Wide-Angle X-ray Scattering (GIWAXS) Characterization were performed at beamline 7.3.3[2] at the Advanced Light Source. Samples were prepared on Si substrates using identical blend solutions as those used in devices.

The 10 keV X-ray beam was incident at a grazing angle of 0.11°-0.15°, selected to maximize the scattering intensity from the samples. The scattered x-rays were detected using a Dectris Pilatus 2M photon counting detector. Contact angles were measured on the neat donor and acceptor films with the contact angle meter (Theta Flex, Biolin) by using two different solvents (water and glycerol).

For femtosecond transient absorption spectroscopy, the fundamental output from Ti: sapphire laser source (800 nm, 100 fs, 1 kHz, Coherent) was separated to two light beam. The stronger one of which was frequency doubled to generate a 400 nm pump light, and the other one was focused into a sapphire plate to generate a broadband supercontinuum probe light. Using an optical chopper, the repetition rate of the pump pulses was adjusted to 500 Hz, and were focused on the sample with the probe pulse (white light). The TA spectra were obtained by comparing the probe light spectra with and without pump light excitation. The photoinduced absorption change as a function of wavelength was described using optical density (absorbance) changes ($\Delta OD(\lambda)$). By adjusting the delay time between the pump and probe pulses, a 3D transient spectral image $\Delta OD(\lambda,t)$ was formed.

The hole and electron mobility were measured using the space charge limited current (SCLC) method, employing a diode configuration of ITO/PEDOT:PSS/active layer/Au for hole and glass/Al/active layer/Al for electron by taking the dark current density in the range of 0-8 V and fitting the results to a space charge limited form, where SCLC is described by:

$$J = \frac{9\varepsilon_0\varepsilon_r\mu_0 V^2}{8L^3}$$

where J is the current density, L is the film thickness of the active layer, μ is the hole or electron mobility, ε_r is the relative dielectric constant of the transport medium, ε_0 is the permittivity of

free space (8.85×10^{-12} F m^{-1}), V (= V_{appl} - V_{bi}) is the internal voltage in the device, where V_{appl} is the applied voltage to the device and V_{bi} is the built-in voltage due to the relative work function difference of the two electrodes.

The current density-voltage (J-V) characteristics of photovoltaic devices were obtained using a Keithley 2400 source-measure unit. The photocurrent was measured under illumination simulated 100 mW cm^{-2} AM1.5G irradiation using a xenon-lamp-based solar simulator [Oriel 96000 (AM1.5G)] in an argon filled glove box. Simulator irradiance was characterized using a calibrated spectrometer and illumination intensity was set using a certified silicon diode. External quantum efficiency (EQE) values of the devices were measured using Stanford Research Systems SR810 lock-in amplifier.

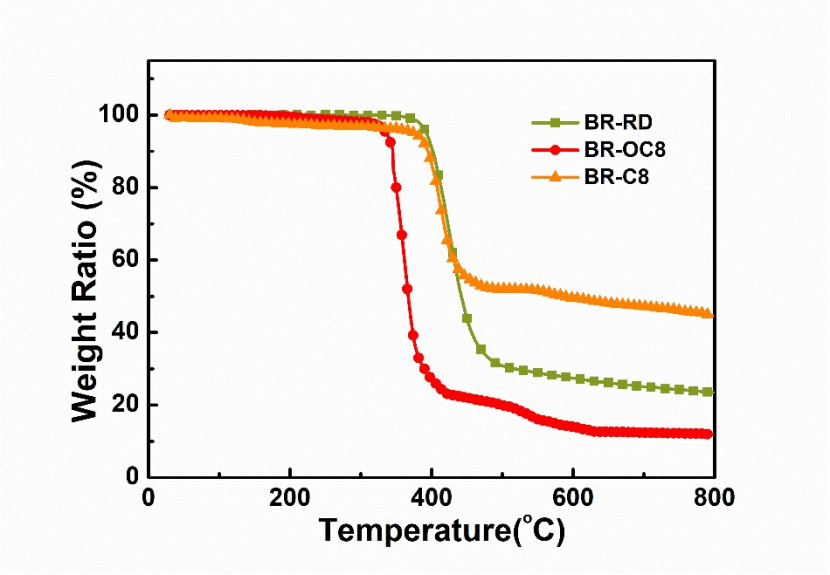

Figure S1. TGA plot of BR-X series.

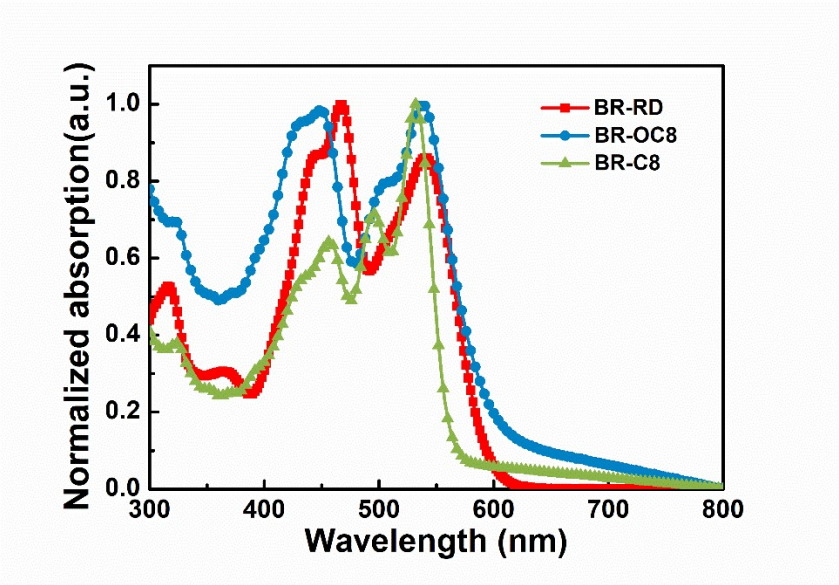

Figure S2. Normalized absorption spectra of BR-RD, BR-OC8 and BR-C8 in chloroform solution.

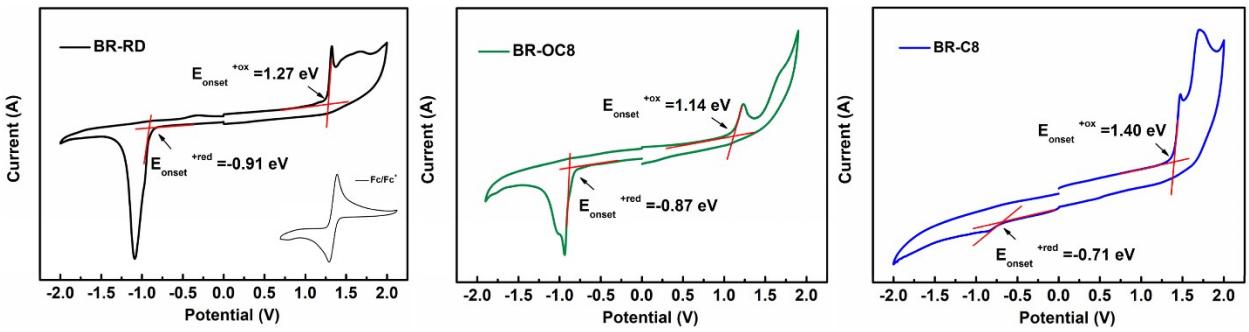

Figure S3. Cyclic voltammograms of BR-RD, BR-OC8, BR-C8 and Fc/Fc^+. The HOMO and LUMO positions are determined by the point of intersection using two tangent lines at the onsets of oxidation or reduction waves. The equation of $E_{LUMO/HOMO} = -e(E_{red/ox}+4.40)$ (eV) was used to calculate the LUMO and HOMO levels (the redox potential of Fc/Fc^+ is found to be 0.40 V).

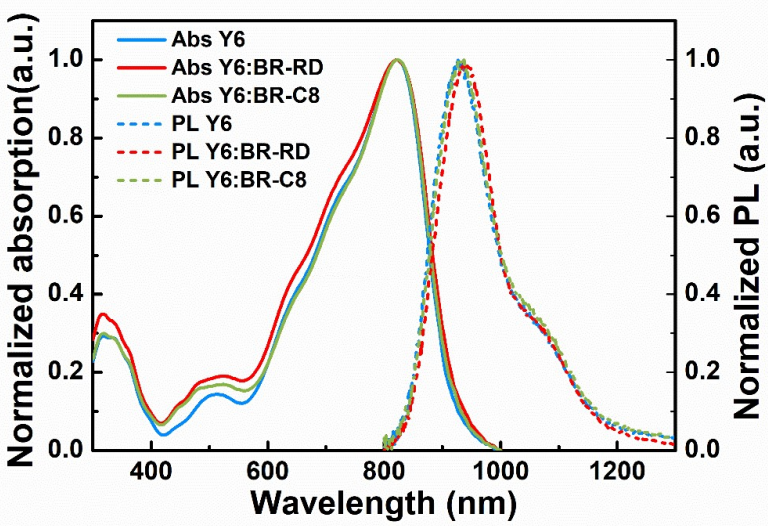

Figure S4. The normalized absorption spectra and PL spectra of neat and blend acceptor films.

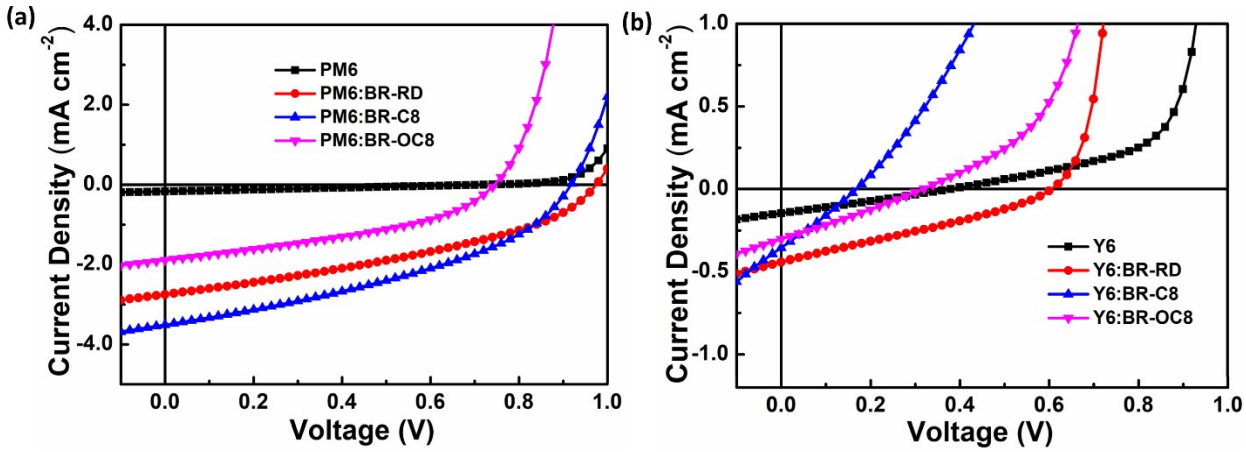

Figure S5. *J*-V curves for the devices based on (a) PM6:BR-X series and (b) Y6:BR-X series.

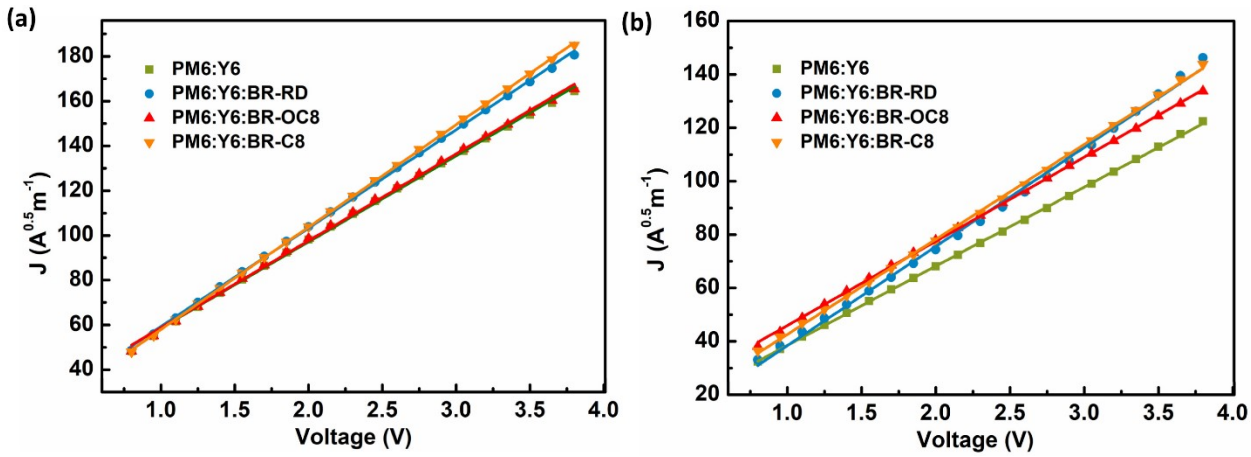

Figure S6. $J^{1/2}$~V characteristics for the devices based on the blend films of PM6:Y6:BR-X series; Solid lines are the fitting lines of the data.

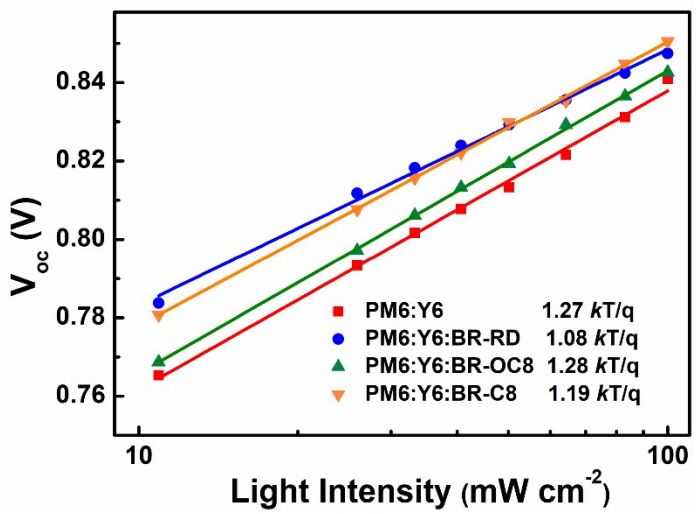

Figure S7. Open-circuit voltage versus light intensity plots of the binary and PM6:Y6:BR-X based ternary devices.

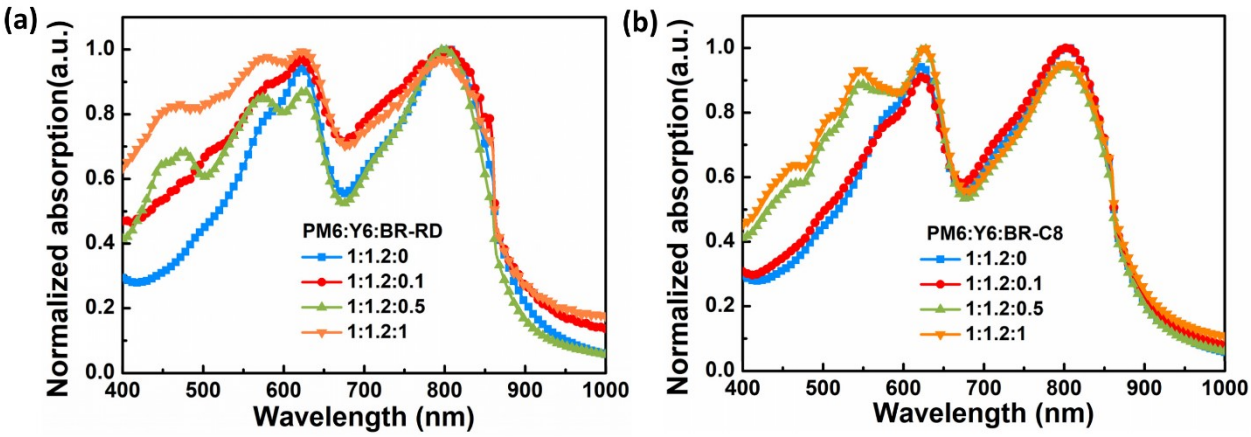

Figure S8. Absorption spectra for (a) PM6:Y6:BR-C8 and (b) PM6:Y6:BR-C8 ternary films with various amounts of ratios.

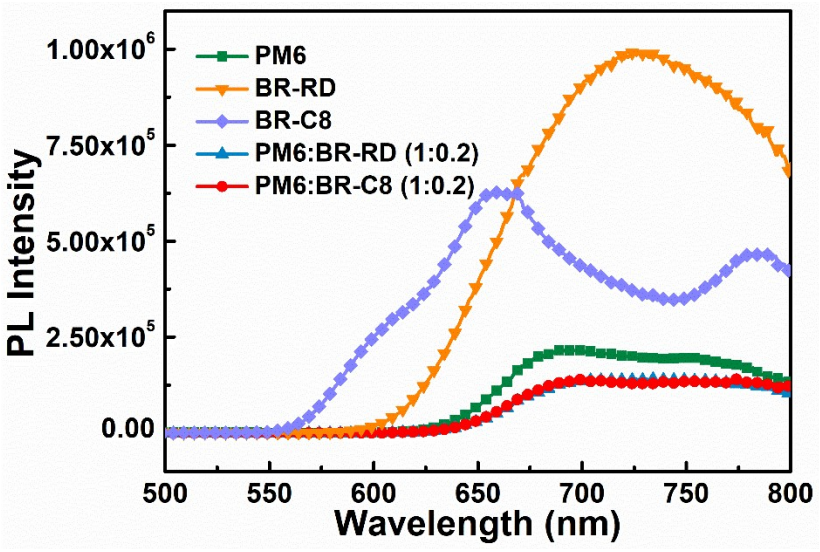

Figure S9. PL spectra excited at 450 nm for PM6, BR-RD, BR-C8, PM6:BR-RD and PM6:BR-C8.

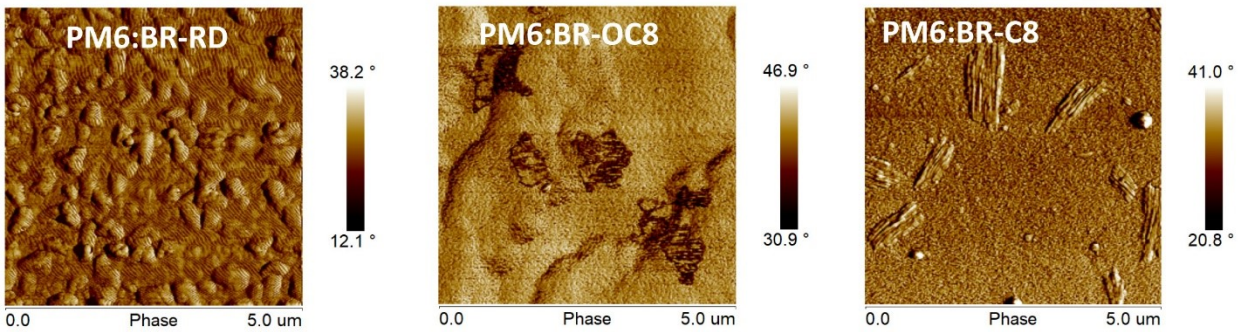

Figure S10. AFM phase images for PM6:BR-RD, PM6:BR-OC8 and PM6:C8.

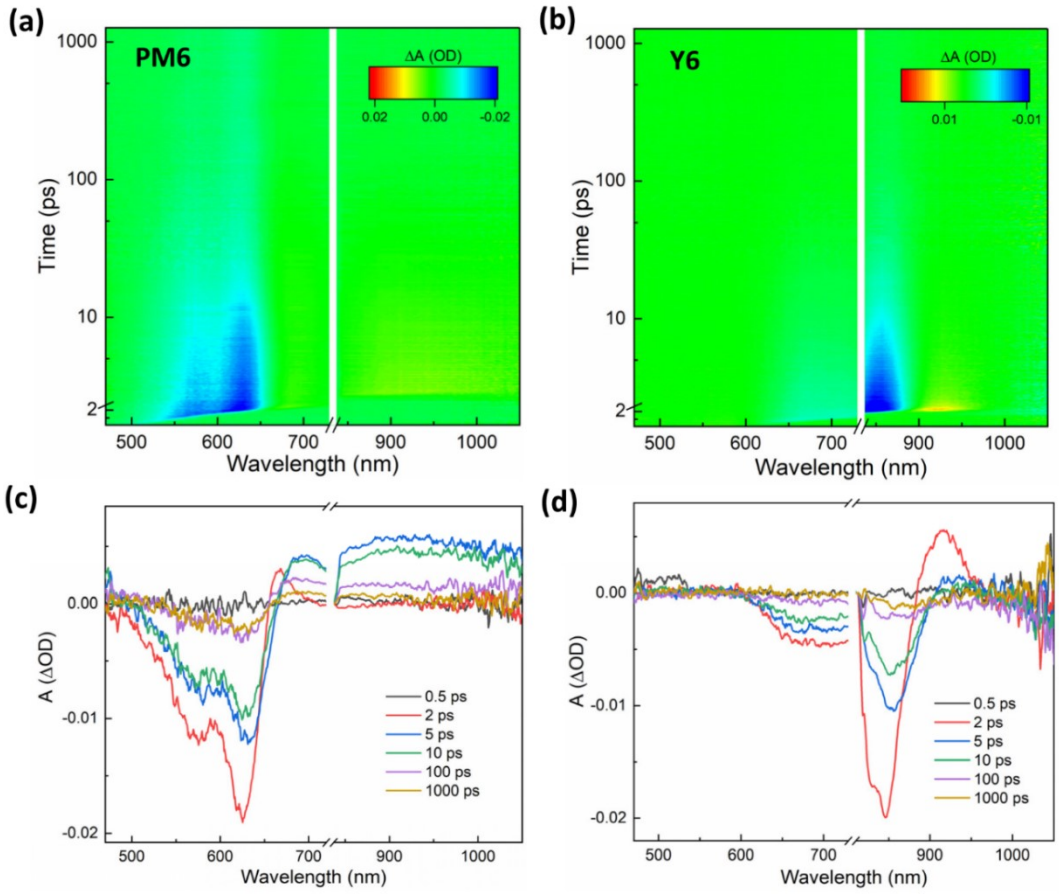

Figure S11. 2D color plot of TA spectra of the (a) PM6 pure film, (b) Y6 pure film. Representative TA spectra of (c) PM6 pure film, (d) Y6 pure film at specific delay times.

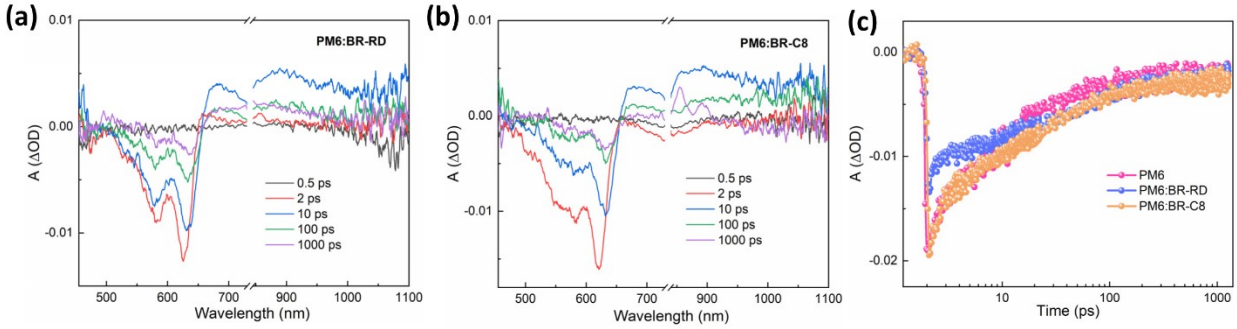

Figure S12. Representative TA spectra of (a) PM6:BR-RD film and (b) PM6:BR-C8 film at specific delay times. (c) dynamics curves probed at 630 nm for PM6 pure film, PM6:BR-RD and PM6:BR-C8 f blend films.

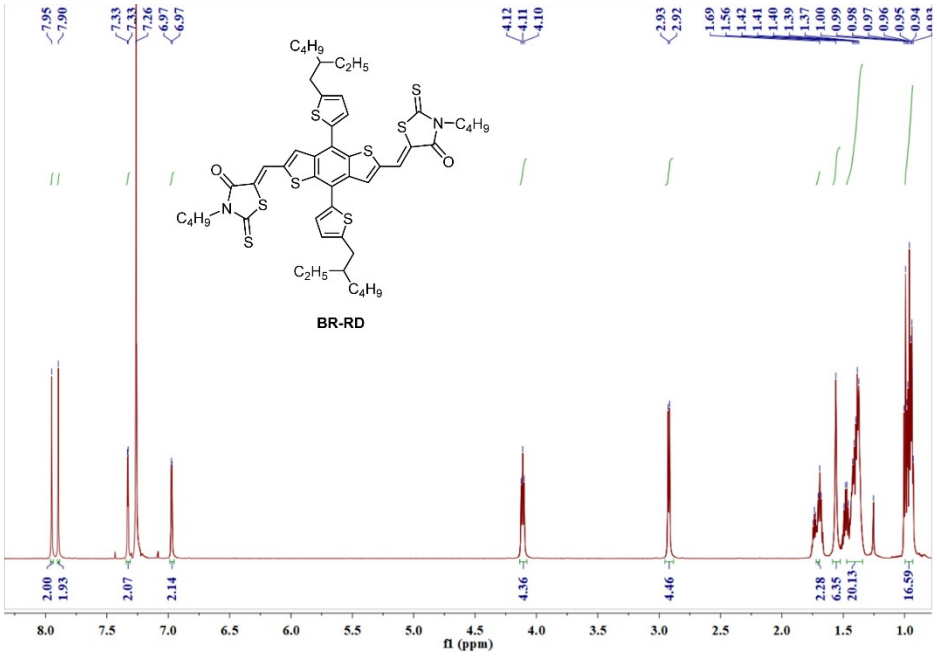

^{1}H NMR spectrum of BR-RD

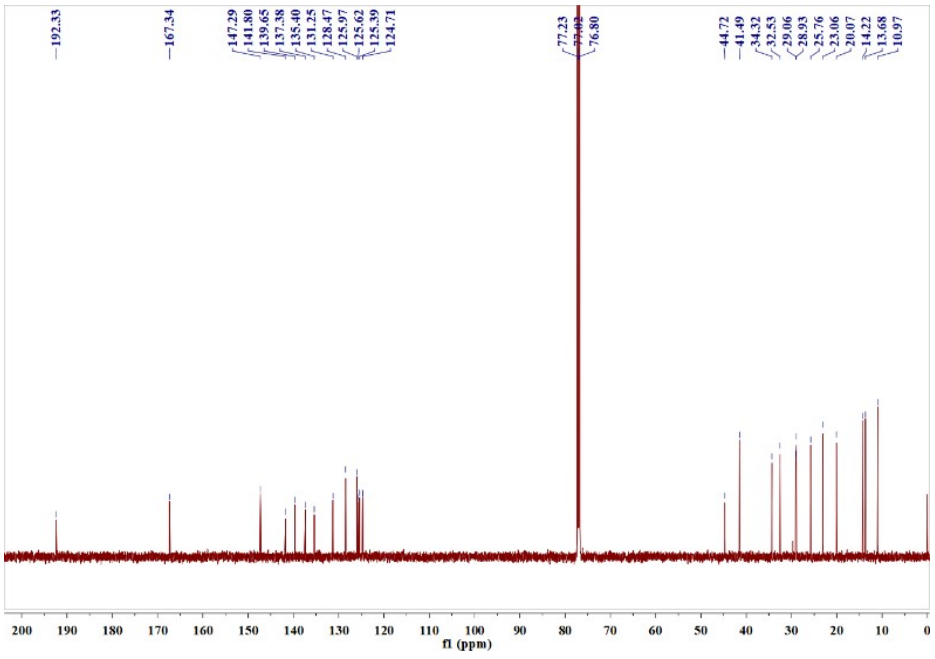

^{13}C NMR spectrum of BR-RD

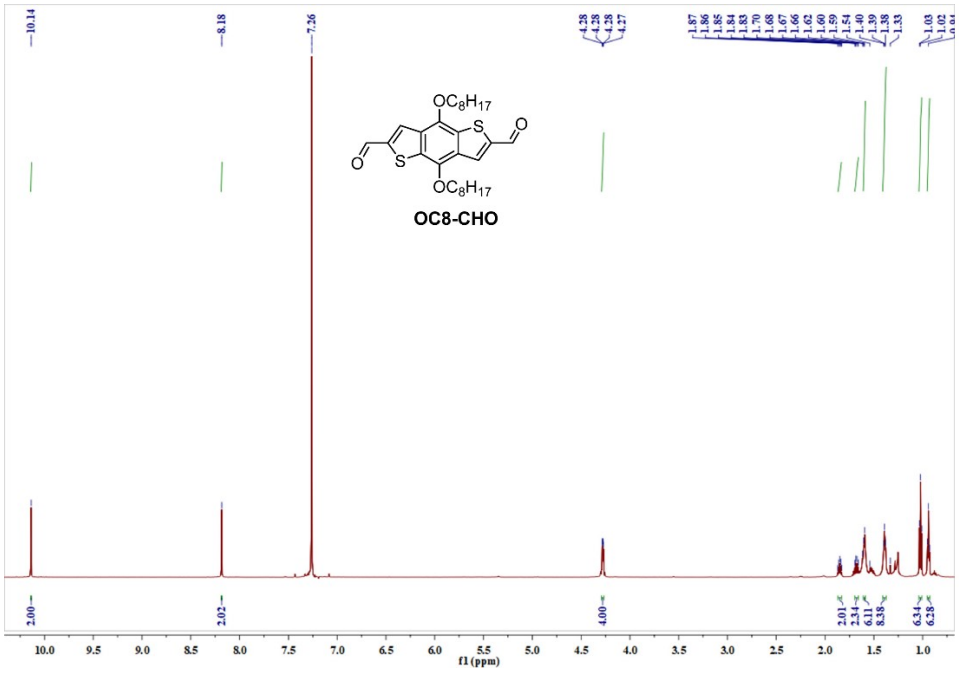

^{1}H NMR spectrum of OC8-CHO

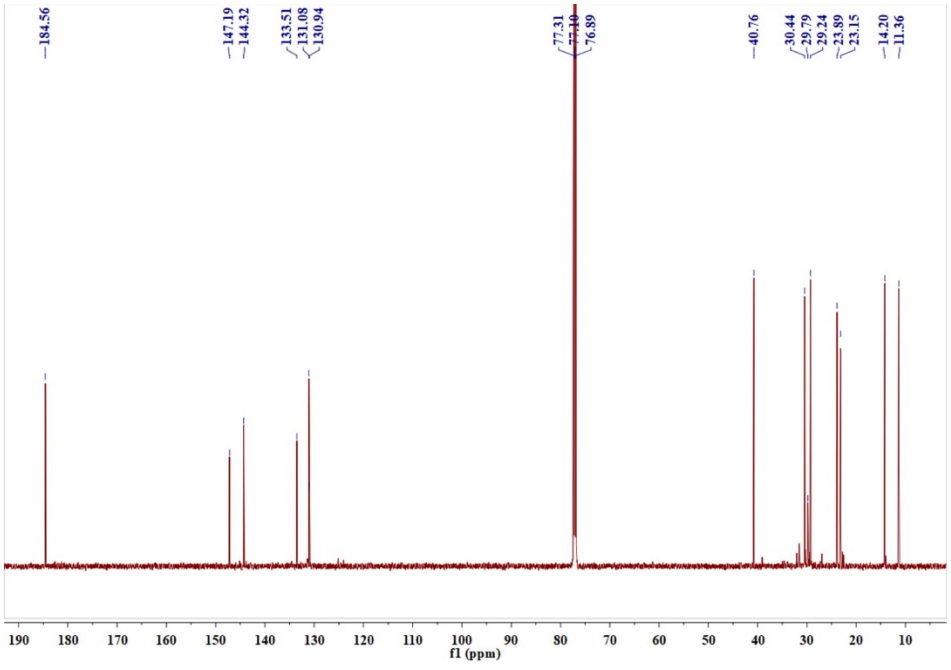

^{13}C NMR spectrum of OC8-CHO

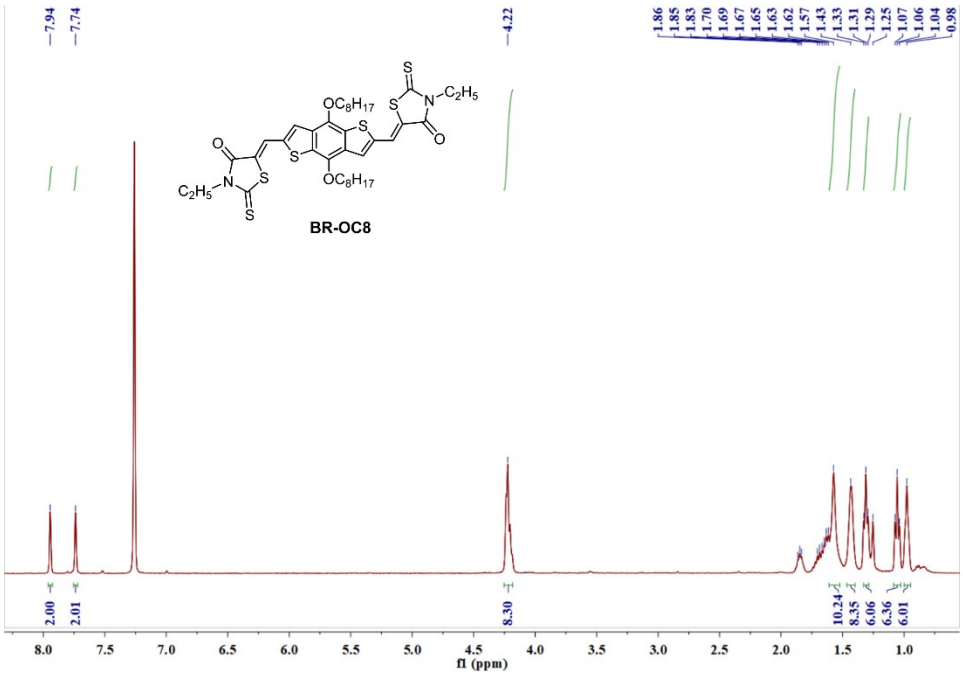

^{1}H NMR spectrum of BR-OC8

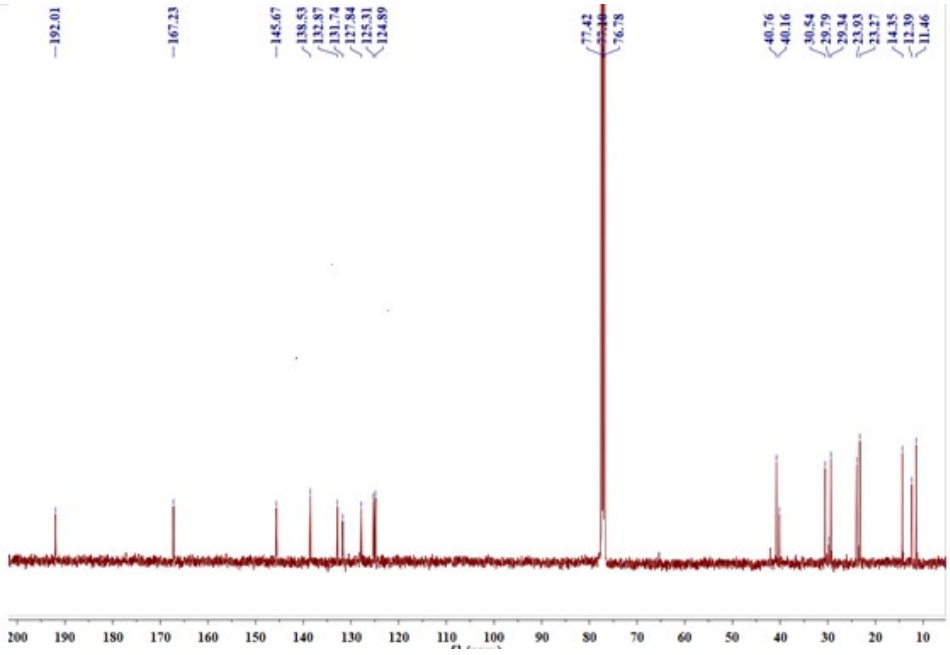

^{13}C NMR spectrum of BR-OC8

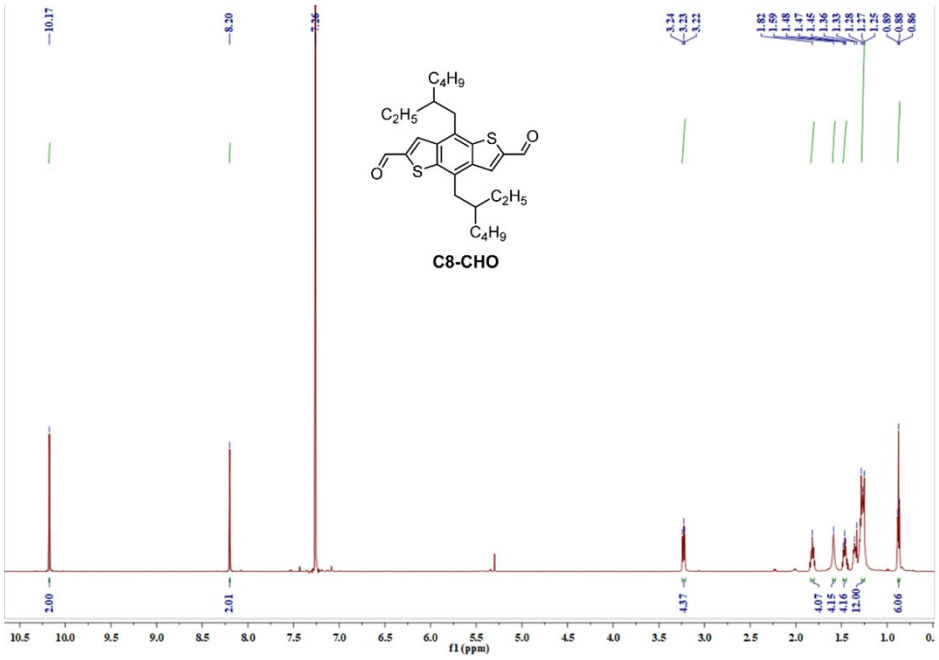

^{1}H NMR spectrum of C8-CHO

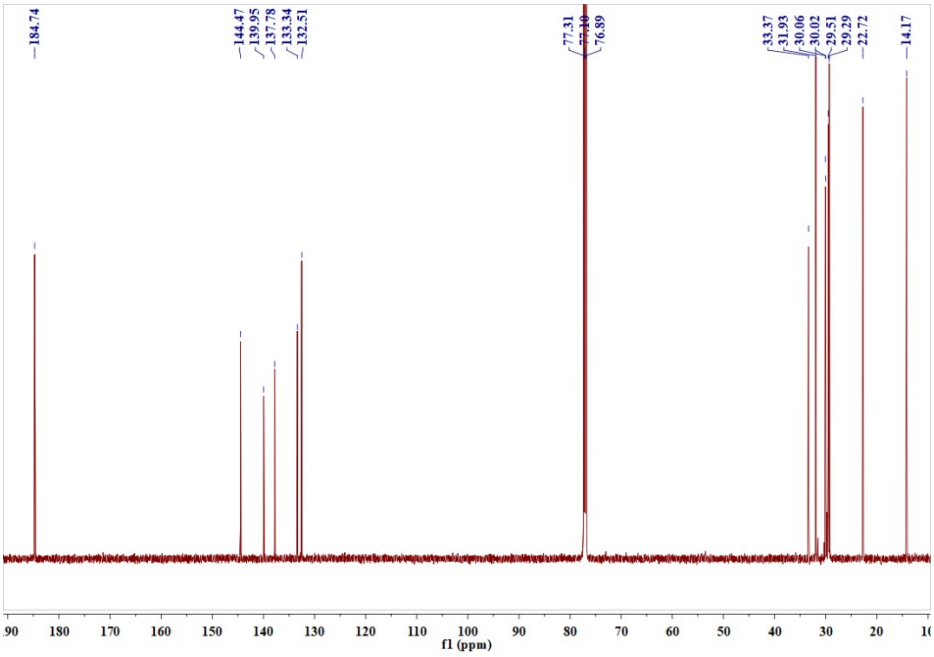

^{13}C NMR spectrum of C8-CHO

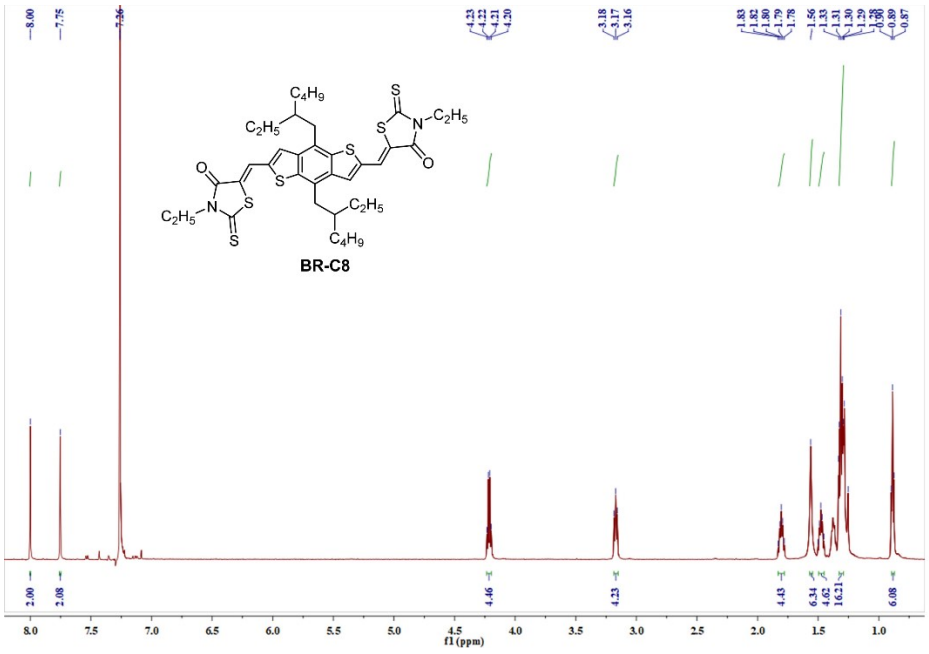

^{1}H NMR spectrum of BR-C8

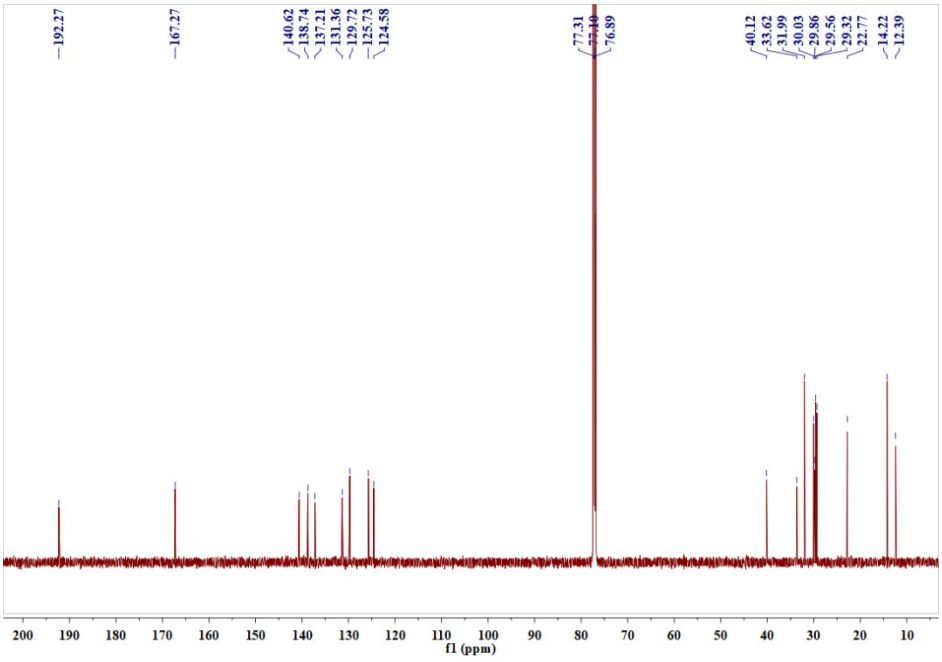

^{13}C NMR spectrum of BR-C8

Figure S13. NMR spectra of the target products.

Table S1. Photovoltaic performance of the solar cells based on PM6:Y6:BR-RD, PM6:Y6:BR-OC8 and PM6:Y6:BR-C8 with different D:A ratio under illumination of AM 1.5 G, 100 mW cm^{-2}.

Blend	Third component ratio (wt%)	V_{oc} (V)	J_{sc} (mA cm^{-2})	FF(%)	PCE (%)
PM6:Y6:BR-RD	5	0.840	26.40	75.7	16.79
	10	0.848	27.28	75.6	17.49
	20	0.852	26.69	76.2	17.33
PM6:Y6:BR-OC8	5	0.841	25.98	75.46	16.48
	10	0.844	26.50	74.7	16.73
	20	0.846	25.84	76.4	16.70
PM6:Y6:BR-C8	5	0.841	26.81	75.4	16.99
	10	0.847	26.94	75.7	17.28
	20	0.851	26.34	75.9	17.02

Table S2. Photovoltaic performance of the PM6:BR-X based organic solar Cells with various BR-X ratios .

Active layer	Ratio	V_{oc} (V)	J_{sc} (mA cm^{-2})	FF(%)	PCE (%)
PM6	-	0.73	0.18	25.6	0.034
PM6:BR-RD	1:0.8	0.98	2.82	34.2	0.94
	1:1	0.97	2.75	37.9	1.01
	1:1.2	0.92	2.29	28.9	0.62
PM6:BR-C8	1:0.8	0.91	3.86	29.0	1.01
	1:1	0.92	3.55	39.1	1.26
	1:1.2	0.90	3.48	29.2	0.92
PM6:BR-OC8	1:0.8	0.74	1.50	33.5	0.38
	1:1	0.75	1.89	39.7	0.56
	1:1.2	0.71	1.22	33.1	0.29

Table S3. Photovoltaic parameters of the Y6:BR-X-based organic solar Cells.

Active layer	V_{oc} (V)	J_{sc} (mA cm^{-2})	FF(%)	PCE (%)
Y6	0.3785	0.15	26.4	0.01
Y6:BR-RD	0.6057	0.44	29.4	0.08
Y6:BR-C8	0.1685	0.35	27.2	0.01
Y6:BR-OC8	0.3171	0.30	27.1	0.03

Table S4. The ratio of J_{sc}/J_{sat} and J_{max}/J_{sat} of binary and ternary devices.

Active layer	J_{sc}/J_{sat}	J_{max}/J_{sat}
PM6:Y6	97.7%	85.3%
PM6:Y6:BR-RD	97.8%	87.5%
PM6:Y6:BR-OC8	97.7%	86.5%
PM6:Y6:BR-C8	97.9%	86.6%

Table S5. Contact angle of water and glycerol and surface tension of PM6, Y6, BR-RD, and BR-C8.

Film	θ_{water} [°]	θ_{GL} [°]	γ [mN m^{-1}]
PM6	101.0	90.8	21.3
Y6	96.6	77.5	29.6
BR-RD	96.6	89.2	23.8
BR-C8	100.5	88.3	22.6

Reference

1. X. Zhang, M. Liu, B. Yang, X. Zhang, Z. Chi, S. Liu, J. Xu and Y. Wei. *Polym. Chem.* 2013, **4**, 5060-5064.

2. A. Hexemer, W. Bras, J. Glossinger, E. Schaible, E. Gann, R. Kirian, A. MacDowell, M. Church, B. Rude and H. Padmore. *J. Phys. Conf. Ser*. 2010, **247**, 012007.